ACS Catalysis

Research Article

Cite This: ACS Catal. 2020, 10, 1146−1151

pubs.acs.org/acscatalysis

Highly Efficient Electrocatalytic Reduction of CO_2 to CO by a Molecular Chromium Complex

Shelby L. Hooe, Julia M. Dressel, Diane A. Dickie, and Charles W. Machan*

Department of Chemistry, University of Virginia, McCormick Road, P.O. Box 400319, Charlottesville, Virginia 22904-4319, United States

Supporting Information

ABSTRACT: Earth-abundant transition-metal catalysts capable of reducing CO_2 to useful products have been gaining attention to meet increasing energy demands and address concerns of rising CO_2 emissions. Group 6 molecular compounds remain underexplored in this context relative to other transition metals. Here, we present a molecular chromium complex with a 2,2′-bipyridine-based ligand capable of selectively transforming CO_2 into CO with phenol as a sacrificial proton donor at turnover frequencies of 5.7 ± 0.1 s^{-1} with a high Faradaic efficiency (96 ± 8%) and a low overpotential (110 mV). To achieve the reported catalytic activity, the parent Cr(III) species is reduced by two electron equivalents, suggesting an approximate d^5 active species configuration. Although previous results have suggested that low-valent species from the Cr/Mo/W triad are nonprivileged for CO_2 reduction in synthetic molecular systems, the results presented here suggest that reactivity analogous to late transition metals is possible with early transition metals.

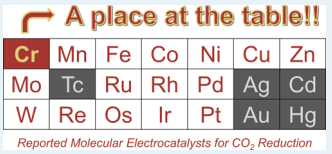

KEYWORDS: *CO_2 reduction, electrocatalysis, molecular, chromium, group 6*

INTRODUCTION

Rising anthropogenic carbon dioxide (CO_2) emissions and atmospheric concentrations continue to drive interest in utilizing renewable energy sources to designate this combustion byproduct as a C_1 synthon.[1,2] In particular, the electrocatalytic reduction of CO_2 into carbon monoxide (CO) is one potential solution, as CO can be a feedstock for light alkanes in a renewable-energy-based Fischer−Tropsch process, if the required H_2 can be generated directly from H_2O.[3,4] Although molecular electrocatalysts for the selective reduction of CO_2 to CO can contain expensive transition metals such as Pd,[5] Ru,[6] and Re,[7] recent developments have focused on earth-abundant transition metals such as Mn,[8,9] Fe,[10] Co,[11] and Ni.[12] It is intriguing that, despite the known role of Mo in the activity of formate[13,14] and carbon monoxide[15] dehydrogenase enzymes, there has been relatively minimal success in the development of active and selective CO_2 reduction electrocatalysts utilizing the Cr/Mo/W triad.[16−22] A d^6 electron configuration is generally thought to be nonprivileged for electrocatalysis under current molecular electrocatalyst "design principles", since the frontier molecular orbitals with sufficient d_{z^2} character and reducing power that are thought to be essential for catalytic activity are easier to access with later transition metals containing redox-active ligands.[23,24]

Kubiak and co-workers showed that Mo and W(bpy-*t*Bu)$(CO)_4$ catalysts, where (bpy-*t*Bu) is 4,4′-di-*tert*-butyl-2,2′-bipyridine, have electrocatalytic activity at reducing potentials under CO_2 saturation conditions; the W derivative was reported to have quantitative Faradaic efficiency for CO (FE_{CO}).[16] In a subsequent study, Hartl and co-workers described the voltammetric response of unfunctionalized bpy analogues of Cr-, Mo-, and W-based tetracarbonyl cores, on Au electrodes,[22] but did not report a FE_{CO}.[20] An additional report by Grice and Saucedo described a catalytic response from $M(CO)_6$ (M = Cr, Mo, W) complexes under reducing conditions, but the FE_{CO} was only reported for Mo.[21] Mo and W catalysts have limited additional reports for electrocatalytic CO_2 reduction, all describing less-than-quantitative efficiency.[25,26]

Herein, we report what is, to our knowledge, the only known Cr homogeneous electrocatalyst with quantitative current efficiencies for the reduction of CO_2 to CO and H_2O.[17,20,21] At catalytic overpotentials of 110 mV, a FE_{CO} of 96 ± 8% is observed over 15.0 turnovers, with negligible H_2 production (<1%). Here, turnover is defined as the passing of charge corresponding to two electron equivalents per catalyst molecule in solution. This unprecedented activity and selectivity are enabled by the unique properties of the ligand framework, which contains a 2,2′-bipyridine backbone with two phenolate moieties. It is worth noting that the observed activity of the Cr catalyst described here is in contrast to the generally accepted design principles that have guided catalyst development for CO_2 reduction over the past 40 years: the selection bias of continued optimization on initial successes has incorrectly suggested that highly reduced mid-to-late transition metals are privileged as molecular electrocatalysts for CO_2 reduction.[23]

Received: October 30, 2019
Revised: December 5, 2019
Published: December 10, 2019

DOI: 10.1021/acscatal.9b04687
ACS Catal. 2020, 10, 1146−1151

RESULTS AND DISCUSSION

The ligand precursor 6,6′-di(3,5-di-*tert*-butyl-2-hydroxybenzene)-2,2′-bipyridine, (^{tbu}dhbpy(H)$_2$) was synthesized by a modified method from our previously reported procedure (see the Supporting Information (SI)).[27] Metalation of (^{tbu}dhbpy(H)$_2$) to generate Cr(^{tbu}dhbpy)Cl(H$_2$O) (**1**) was achieved at room temperature by stirring overnight (^{tbu}dhbpy(H)$_2$) with 1 equiv of chromium(II) dichloride in tetrahydrofuran (THF) under an inert atmosphere, followed by exposure to air (SI). The purified product was characterized by UV−vis (Figure S1), NMR (Table S1), electrospray ionization-mass spectrometry (ESI-MS) (Figure S2), microanalysis (SI), and single-crystal X-ray diffraction (XRD) studies (Figure 1). Crystals suitable for XRD studies were grown via room-temperature evaporation of a concentrated solution of **1** in a mixture of dichloromethane and acetonitrile (MeCN) (Figure 1).

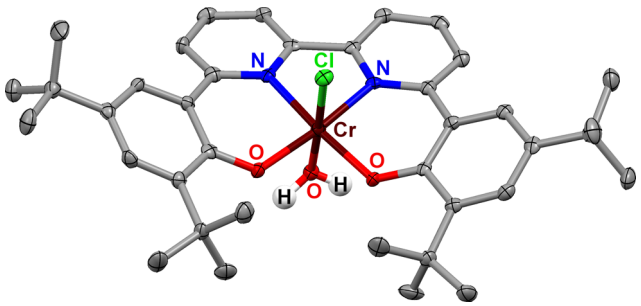

Figure 1. Molecular structure of Cr(^{tbu}dhbpy)Cl(H$_2$O) (**1**) obtained from single-crystal X-ray diffraction studies. Blue = N, red = O, gray = C, green = Cl, maroon = Cr, white = H atoms of bound water molecule; thermal ellipsoids at 50%; ligand H atoms and occluded MeCN molecule omitted for clarity; hydrogen atoms of the Cr-bound water molecule were located in the diffraction map and refined isotropically.

Cyclic voltammetry (CV) experiments were performed on Cr(^{tbu}dhbpy)Cl(H$_2$O) (**1**) in dimethylformamide (DMF) with 0.1 M tetrabutylammonium hexafluorophosphate (TBAPF$_6$) as the supporting electrolyte. Under argon (Ar) saturation conditions, three redox features are observed with E_p = −1.66 and −1.78 V and $E_{1/2}$ = −1.95 V versus the ferrocenium/ferrocene (Fc$^+$/Fc) reduction potential (Figure 2, black). Under CO$_2$ saturation conditions in the presence of a proton source, catalysis for CO$_2$ reduction mediated by **1** was observed at the third redox feature, $E_{1/2}$ = −1.95 V versus Fc$^+$/Fc, vide infra (Figure 2, green). Using tetrabutylammonium chloride (TBACl) as a source of excess anions, the dissociation of Cl$^-$ upon electrochemical reduction of **1** was analyzed (Figures S3 and S4). Under Ar saturation conditions, the addition of TBACl causes a shift toward more negative potentials at the first redox feature (Figure S3A); interestingly, this shift is less significant under identical conditions in the presence of phenol (PhOH) (Figure S3B). These results are similar to those observed under CO$_2$ (Figure S4A). This suggests that the first two redox features are related to one another and that the feature at more positive potentials is likely to be a solvento species resulting from an equilibrium chloride displacement reaction. Additionally, only 1.9 equiv of charge were passed at a potential of −2.3 V versus Fc$^+$/Fc during a coulometry experiment with **1** under an inert atmosphere (Figure S5). This suggests that the active catalyst species of **1** is generated via a two-electron reduction. Consistent with this, variable scan rate dependence studies show a coalescence of the first and second reduction waves at scan rates of ≥2000 mV/s (Figure S6). Therefore, we ascribe these first two waves as representing the end states of a chloride dissociation equilibrium involving the parent Cr(III) species.

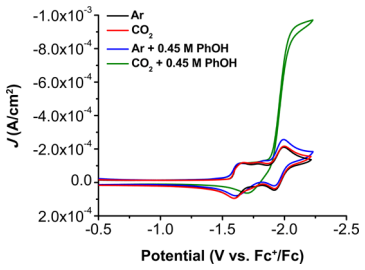

Figure 2. Comparison of CVs under Ar and CO$_2$ saturation conditions with and without 0.45 M PhOH. Conditions: 1.0 mM analyte in 0.1 M TBAPF$_6$/DMF; glassy carbon working electrode, glassy carbon rod counter electrode, Ag/AgCl pseudoreference electrode; referenced to Fc$^+$/Fc internal standard; 100 mV/s scan rate.

Upon the addition of PhOH as a proton donor under Ar saturation conditions, only minor shifts in potential and changes in current are observed (Figure 2, blue). In previous studies, we have shown that this ligand framework undergoes a multisite proton-coupled electron-transfer reaction under reducing conditions with an added proton donor, where reduction of Mn and Fe metal centers causes protonation of the metal-coordinated O atoms.[27−29] Unlike the previous cases, no clear Nernstian dependence on the concentration of added proton donor is observed, suggesting that formal protonation of the Cr-bound O atoms does not occur to the extent which it was previously observed for related Fe and Mn derivatives.[27−29] There are, however, changes in the CV response consistent with an interaction between the added PhOH and the reduced Cr species, which we tentatively assign as the result of a noncovalent interaction between the proton donor and the reduced catalyst.[30,31]

Under CO$_2$ saturation conditions without PhOH present, minimal changes are observed in the CV response compared to that under Ar saturation conditions (Figure 2, red). Variable scan rate studies under both Ar (Figure S6) and CO$_2$ (Figure S7) saturation demonstrate that the third, reversible reduction feature at $E_{1/2}$ = −1.95 V versus Fc$^+$/Fc is diffusion controlled, indicative of a homogeneous electrochemical response (Figures S6 and S7). Under CO$_2$ saturation conditions with added PhOH, a large increase in current is observed at the third reduction feature in the form of an irreversible wave with a distinct plateau (Figure 2, green). To probe the electrochemical reaction taking place and develop a catalytic rate expression, variable concentration studies were performed under these conditions. By titrating PhOH into a CO$_2$ saturated solution of **1**, the logarithmic relationship between the increase in current and the PhOH concentration can be used to determine the order for the reaction with respect to the proton donor (Figure S8).[32] Similar studies were done by varying the concentrations of CO$_2$ (Figure 3) and catalyst (Figure S9). The electrochemical reaction under these conditions was found to have a first-order concentration dependence with respect to PhOH (Figure S8), complex **1** (Figure S9), and CO$_2$ (Figure 3).[32]

DOI: 10.1021/acscatal.9b04687
ACS Catal. 2020, 10, 1146−1151

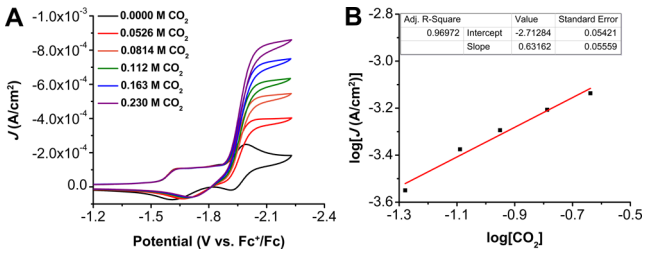

Figure 3. (A) CVs of Cr(^{tbu}dhbpy)Cl(H_2O) **1** obtained under variable CO_2 concentration with 0.36 M PhOH. Conditions: 1.0 mM analyte with 0.1 M $TBAPF_6$/DMF; glassy carbon working electrode, glassy carbon counter electrode, Ag/AgCl pseudoreference electrode; 100 mV/s scan rate; referenced to internal ferrocene standard. (B) Log−log plot from data obtained from CVs of Cr(^{tbu}dhbpy)Cl(H_2O) **1** (1.0 mM) under variable CO_2 concentration conditions with 0.36 M PhOH.

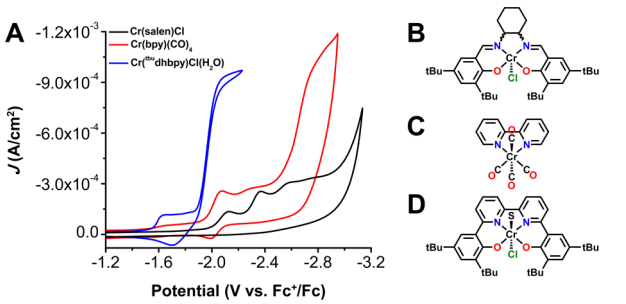

Figure 4. (A) Comparison of CVs for different Cr complexes under CO_2 saturation conditions: 0.22 M PhOH (black) with the Cr(salen)Cl complex (B), 1.32 M PhOH (red) with the Cr(bpy)-$(CO)_4$ complex (C), and 0.34 M PhOH (blue) with **1** (D), where S is a solvento adduct of water or DMF. Conditions: 1.0 mM analyte in 0.1 M $TBAPF_6$/DMF; glassy carbon working electrode, glassy carbon rod counter electrode, Ag/AgCl pseudoreference electrode; referenced to Fc^+/Fc from either ferrocene or decamethylferrocene internal standard; 100 mV/s scan rate.

Controlled potential electrolysis (CPE) was performed at −2.1 V versus Fc^+/Fc with 0.62 M PhOH under CO_2 saturation conditions (Figure S10). Gaseous products were assessed by gas chromatography (GC) to quantify the amount of product produced (Figure S11). The results of this experiment (Table S2) showed that **1** was capable of reducing CO_2 to CO under these conditions with 96 ± 8% FE_{CO} over 15.0 turnovers (turnover represents two electron equivalents of charge passed for each equivalent of **1** in solution). As a control for catalyst degradation producing a catalytically active species, the working electrode from this experiment was rinsed with DMF and air-dried. Subsequently, the electrolysis chamber was prepared again with the catalyst omitted under otherwise analogous conditions. Compared to the CPE experiment with **1** present, approximately 22-fold less current was observed at −2.1 V versus Fc^+/Fc with analogous PhOH and CO_2 concentrations; the observed amounts of CO were below the detection limit of the instrument and H_2 was observed with a FE_{H2} of 4 ± 3% (Figure S12). The data obtained from this "rinse test" were comparable in terms of charge passed and products produced to that obtained in an additional control CPE experiment in the absence of **1** with a freshly polished electrode under CO_2 saturation conditions with added PhOH (Figure S13). These data are consistent with the proposal that **1** is a precatalyst for a molecular catalytic response. In parallel, results from a CV rinse test showed no apparent adsorption onto the electrode surface during catalytic CV experiments in the presence of **1** (Figure S14).

The electrocatalytic performance observed for **1**, FE_{CO} (96 ± 8%) and low overpotential (110 mV), represents a profound advancement over the known molecular Cr electrocatalysts for CO_2 reduction.[16,18,20−22,24−26] To further demonstrate this, we prepared partial structural analogues Cr(bpy)$(CO)_4$[33] and the Cr salen complex *N*,*N*′-bis(3,5-di-*tert*-butylsalicylidene)-1,2-cyclohexanediaminochromium(III) chloride (mixture of *R*,*R* and *S*,*S* isomers), Cr(salen)Cl,[34] for a comparative study (Figure 4, see the SI). CV experiments under Ar saturation conditions with the Cr(salen)Cl complex showed four irreversible redox features with E_p = −2.18, −2.46, −2.59, and −2.95 V versus Fc^+/Fc (Figure S15, black). The Cr(bpy)$(CO)_4$ complex exhibited two redox features, one reversible with $E_{1/2}$ = −2.03 and one irreversible with E_p = −2.64 V versus Fc^+/Fc (Figure S16, black). Under CO_2 saturation conditions, a slight increase in current is observed for the Cr(salen)Cl in the absence of a sacrificial proton donor (Figure S15, red). Upon the addition of PhOH under both Ar and CO_2 saturation conditions, minimal current changes are observed with Cr(salen)Cl present; a shift toward positive potentials is observed under both Ar and CO_2 saturation conditions for the first two reduction features (Figure S15).

Under CO_2 saturation conditions, CVs of the Cr(bpy)-$(CO)_4$ complex demonstrate minimal reactivity in comparison to the experiments conducted with Ar present (Figure S16). Interestingly, upon the addition of PhOH under CO_2 saturation conditions, increases in current are observed (Figure S16, blue). However, the Cr(bpy)$(CO)_4$ complex shows that current increases under both Ar and CO_2 saturation conditions with PhOH present, suggesting limited selectivity for CO_2 (Figure S16). Less-than-quantitative amounts of CO and H_2 were detected in CPE experiments performed to assess the possibility of catalytic CO_2 reduction with the Cr(salen)Cl (Figure S17) and Cr(bpy)$(CO)_4$ (Figure S18) complexes and both appeared to degrade over time during the electrolysis (Table S3). The described CPE results and CV comparison (Figure 4A) of the three Cr complexes (Figure 4B−D) suggest that **1** displays unique redox and electrocatalytic activity for CO_2 reduction compared to Cr(salen)Cl and Cr(bpy)$(CO)_4$.

Variable scan rate methods were used to establish where the catalytic reaction becomes independent of scan rate for **1** (Figures S19 and S20 and Table S4).[35] CV data obtained at scan rates from 25 to 5000 mV/s under catalytic and Faradaic conditions were used to show that a scan-rate-independent regime is achieved between 200 and 1000 mV/s. TOF_{MAX} values were calculated using the ratio of i_{cat}/i_p at each scan rate across this range, suggesting an average TOF_{MAX} of 5.7 ± 0.1 s^{-1} at a catalytic overpotential of 110 mV (see Figure S20 for the determination of TOF_{MAX}).

CO_2 reduction mechanisms that produce CO could have two possible rate-defining steps: (i) CO_2 binding and (ii) C−OH bond cleavage.[23,24] Overwhelmingly, mechanistic proposals for molecular catalysts center on C−OH bond cleavage as the rate-determining step because of the kinetic constraints imposed by heavy atom bond cleavage.[23,24] Given that the Cr(III) catalyst is activated by only two overall electron equivalents to a putative d^5 state, we were interested in specifically excluding the possibility of CO_2 binding as the rate-determining step. Using the experimentally determined

DOI: 10.1021/acscatal.9b04687
ACS Catal. 2020, 10, 1146−1151

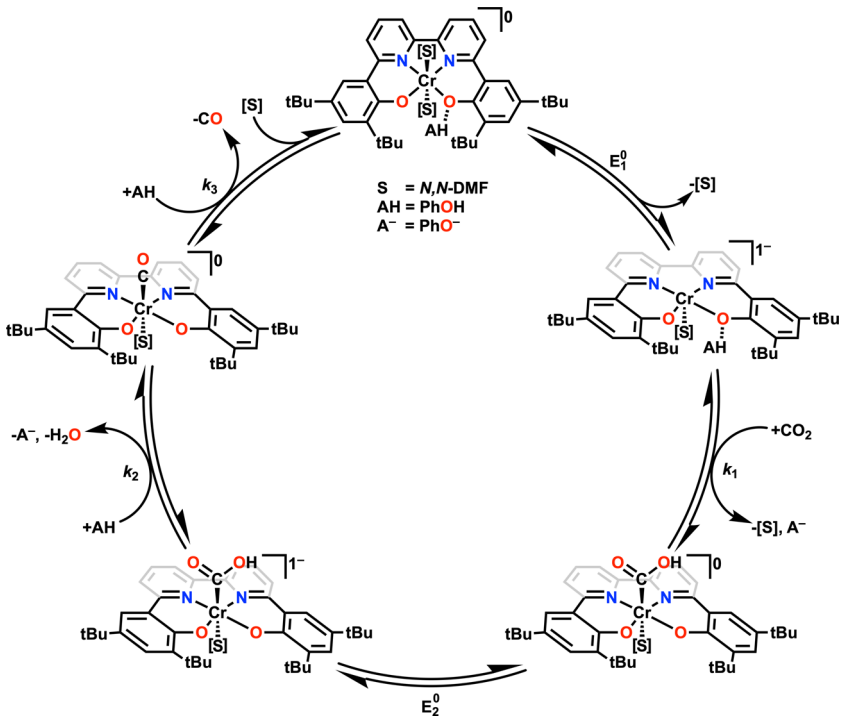

Figure 5. Proposed mechanistic cycle for the reduction of CO_2 by **1** in DMF with PhOH as the proton donor. [S] indicates possible but speculative assignments for DMF solvento species that were not considered in the CV simulations.

diffusion coefficient from variable scan rate studies of **1** (Figure S21), digital CV simulations were simultaneously fit to five experimental catalytic data sets in the scan rate-independent regime from 50 to 300 mV/s (Figures 6 and S22 and Table S5). For simplicity, only the final reduction wave, from which the catalytic response originates, was modeled (SI). According to this analysis, the overall reaction follows an *ECEC* (*E*, electrochemical step; *C*, chemical step) mechanism, where reduction and chemical steps follow one another in sequence. The complete proposed cycle from the singly reduced $[Cr(^{tbu}dhbpy)][AH]^0$ state, where [AH] is an equivalent of PhOH in a noncovalent interaction with the ligand O atoms of the neutral Cr precatalytic intermediate, is summarized below (eqs 1−5 and Figure 5). Given the low electron count at the Cr center for this complex, we cannot exclude that many of these species may exist as mono- or disolvento DMF adducts and have indicated speculative speciation assignments in Figure 5.

$$[[Cr(L)][AH]]^0 + e^- \overset{E_1^0}{\rightleftharpoons} [[Cr(L)][AH]]^- \quad (1)$$

$$[Cr(L)][AH]^- + CO_2 \overset{k_1}{\rightarrow} [Cr(L)(CO_2H)]^0 + A^- \quad (2)$$

$$[Cr(L)(CO_2H)]^0 + e^- \overset{E_2^0}{\rightleftharpoons} [Cr(L)(CO_2H)]^- \quad (3)$$

$$[Cr(L)(CO_2H)]^- + AH \overset{k_2}{\rightarrow} [Cr(L)(CO)]^0 + A^- + H_2O \quad (4)$$

$$[Cr(L)(CO)]^0 + AH \overset{k_3}{\rightarrow} [[Cr(L)][AH]]^0 + CO \quad (5)$$

As indicated above, modeling the catalytic wave across five separate scan rates was consistent with the experimentally observed TOF_{MAX} arising from k_2, the proposed C−OH bond cleavage step: 6.8 s^{-1} compared to 5.7 ± 0.1 s^{-1} for the experimental TOF_{MAX} (Figure 6). Alternate mechanistic simulations following an *ECCE*-type mechanism were consistent with k_1 as the rate-determining step, but predicted that CO release from the Cr center was not favored, with a K_{eq} of 7.3×10^{-3}. This mechanism could be excluded as a possibility based on the experimental observation that no Nernstian voltammetric response indicative of an equilibrium CO binding reaction was observed at any relevant reduction feature of **1** (Figure S23). Using the reaction parameters obtained from the simulation of the *ECEC* mechanism above, additional CV simulations were used to assess the agreement with the experimental studies on the catalytic current dependence of the added PhOH concentration. Fitting the rate constant for k_2 across different PhOH concentrations using the values in Table S4 validated the assignment of the first-order concentration dependence of the catalytic current on added PhOH (Figure S24): a linear slope of 1.01 was

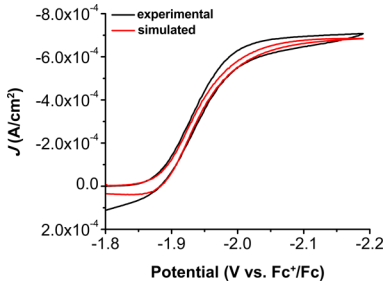

Figure 6. Comparison of simulated (red) and experimental (black) CVs with 1.0 mM $Cr(^{tbu}dhbpy)Cl(H_2O)$ **1**, obtained under CO_2 saturation conditions with 0.341 M PhOH concentration at 100 mV/s. Conditions: 0.1 M $TBAPF_6$/DMF; glassy carbon working electrode, glassy carbon counter electrode, Ag/AgCl pseudoreference electrode; referenced to internal ferrocene standard.

DOI: 10.1021/acscatal.9b04687
ACS Catal. 2020, 10, 1146−1151

obtained from a plot comparing log([PhOH]) against log(k_2(s^{-1})) (note that the apparent turnover frequency at each concentration was calculated from the simulated second-order rate constants; Figure S25).[36]

CONCLUSIONS

We have established that **1** is active and selective as a molecular catalyst for the electrochemical reduction of CO_2 to CO with excellent stability. To our knowledge, no prior study of electrocatalytic behavior for a molecular Cr species has achieved the performance reported here. Although the observed turnover frequency of 5.7 ± 0.1 s^{-1} is modest relative to those of other molecular electrocatalysts, such as those based on [Fe(tetraphenylporphyrin)]$^+$ and M(bpy)-$(CO)_3$X (where M = Re or Mn; X = Br or Cl),[9,37−40] we believe that with further study, the activity of this Cr-based catalyst can be further improved. Because of their intermediate d-electron count, group 6 metals have been thought of as poor candidates for developing molecular electrocatalysts for CO_2 reduction; to this point, all catalyst reports for the Cr/Mo/W triad have invoked negative valency or reduction of a ligand framework to achieve a catalytic response.[16−23,25,26] A key aspect of the activity reported here may be that the low electron count achieved at Cr during catalyst activation (d^5) facilitates rapid CO release, which is indirectly observed by the absence of interactions between CO and reduced Cr species observed experimentally in control CVs (Figure S23). We also note with interest that this d-electron count assumes minimal participation of the bpy backbone, which is unlikely to be rigorously true; investigations to further elucidate the electronic structure of the active species are currently underway. The unique catalytic response of this molecular Cr complex represents an entry point into active and selective transition-metal electrocatalysts from group 6 and earlier, which to this point have been extremely rare.[10,24,37−41]

ASSOCIATED CONTENT

Supporting Information

The Supporting Information is available free of charge at https://pubs.acs.org/doi/10.1021/acscatal.9b04687.

Full experimental details, detailed synthetic procedures, electrochemical characterizations, digital CV simulation, and product quantification; UV−vis serial dilution absorbance data; ESI-MS characterization of Cr-(tbudhbpy)Cl(H_2O) **1**; current versus time trace from bulk electrolysis experiment; and comparison of simulated and experimental CV with 1.0 mM Cr-(tbudhbpy)Cl(H_2O) **1** (PDF)

Cr_tBu_dhbpy_Cl_H_2O (CIF)

AUTHOR INFORMATION

Corresponding Author

*E-mail: machan@virginia.edu.

ORCID

Diane A. Dickie: 0000-0003-0939-3309

Charles W. Machan: 0000-0002-5182-1138

Author Contributions

C.W.M. conceived and supervised the experiments; S.L.H. and J.M.D. conducted all experiments; D.A.D. collected and refined X-ray crystallographic data; and C.W.M. and S.L.H. wrote the manuscript.

Notes

The authors declare no competing financial interest.

ACKNOWLEDGMENTS

The authors thank Dr. Vagulejan Balasanthiran for providing the *N*,*N*′-bis(3,5-di-tert-butylsalicylidene)-1,2-cyclohexanediammine ligand as a mixture of *R*,*R* and *S*,*S* isomers. We thank the University of Virginia for generous funding and infrastructural support.

REFERENCES

(1) Ballivet-Tkatchenko, D.; Camy, S.; Condoret, J. S. Carbon Dioxide, a Solvent and Synthon for Green Chemistry. In *Environmental Chemistry: Green Chemistry and Pollutants in Ecosystems*; Lichtfouse, E.; Schwarzbauer, J.; Robert, D., Eds.; Springer: Berlin, Heidelberg, 2005; pp 541−552.

(2) *Global Warming of 1.5°C. An IPCC Special Report*; World Meterological Organization: Geneva, Switzerland, 2018. https://www. ipcc. ch/sr15/ (accessed 2019-10-01).

(3) Jacobs, G.; Davis, B. H. Conversion of Biomass to Liquid Fuels and Chemicals via the Fischer−Tropsch Synthesis Route. In *Thermochemical Conversion of Biomass to Liquid Fuels and Chemicals*; The Royal Society of Chemistry, 2010; Vol. *1*, pp 95−124.

(4) Seh, Z. W.; Kibsgaard, J.; Dickens, C. F.; Chorkendorff, I.; Nørskov, J. K.; Jaramillo, T. F. Combining theory and experiment in electrocatalysis: Insights into materials design. *Science* **2017**, *355*, No. eaad4998.

(5) Raebiger, J. W.; Turner, J. W.; Noll, B. C.; Curtis, C. J.; Miedaner, A.; Cox, B.; DuBois, D. L. Electrochemical Reduction of CO2 to CO Catalyzed by a Bimetallic Palladium Complex. *Organometallics* **2006**, *25*, 3345−3351.

(6) Chen, Z.; Chen, C.; Weinberg, D. R.; Kang, P.; Concepcion, J. J.; Harrison, D. P.; Brookhart, M. S.; Meyer, T. J. Electrocatalytic reduction of CO2 to CO by polypyridyl ruthenium complexes. *Chem. Commun.* **2011**, *47*, 12607−12609.

(7) Wong, K.-Y.; Chung, W.-H.; Lau, C.-P. The effect of weak Brönsted acids on the electrocatalytic reduction of carbon dioxide by a rhenium tricarbonyl bipyridyl complex. *J. Electroanal. Chem.* **1998**, *453*, 161−170.

(8) Sampson, M. D.; Nguyen, A. D.; Grice, K. A.; Moore, C. E.; Rheingold, A. L.; Kubiak, C. P. Manganese Catalysts with Bulky Bipyridine Ligands for the Electrocatalytic Reduction of Carbon Dioxide: Eliminating Dimerization and Altering Catalysis. *J. Am. Chem. Soc.* **2014**, *136*, 5460−5471.

(9) Smieja, J. M.; Sampson, M. D.; Grice, K. A.; Benson, E. E.; Froehlich, J. D.; Kubiak, C. P. Manganese as a Substitute for Rhenium in CO2 Reduction Catalysts: The Importance of Acids. *Inorg. Chem.* **2013**, *52*, 2484−2491.

(10) Azcarate, I.; Costentin, C.; Robert, M.; Savéant, J.-M. Through-Space Charge Interaction Substituent Effects in Molecular Catalysis Leading to the Design of the Most Efficient Catalyst of CO2-to-CO Electrochemical Conversion. *J. Am. Chem. Soc.* **2016**, *138*, 16639−16644.

(11) Cometto, C.; Chen, L.; Lo, P.-K.; Guo, Z.; Lau, K.-C.; Anxolabéhère-Mallart, E.; Fave, C.; Lau, T.-C.; Robert, M. Highly Selective Molecular Catalysts for the CO2-to-CO Electrochemical Conversion at Very Low Overpotential. Contrasting Fe vs Co Quaterpyridine Complexes upon Mechanistic Studies. *ACS Catal.* **2018**, *8*, 3411−3417.

(12) Froehlich, J. D.; Kubiak, C. P. Homogeneous CO2 Reduction by Ni(cyclam) at a Glassy Carbon Electrode. *Inorg. Chem.* **2012**, *51*, 3932−3934.

(13) Reda, T.; Plugge, C. M.; Abram, N. J.; Hirst, J. Reversible interconversion of carbon dioxide and formate by an electroactive enzyme. *Proc. Natl. Acad. Sci. U.S.A.* **2008**, *105*, 10654−10658.

(14) Leopoldini, M.; Chiodo, S. G.; Toscano, M.; Russo, N. Reaction Mechanism of Molybdoenzyme Formate Dehydrogenase. *Chem. - Eur. J.* **2008**, *14*, 8674−8681.

DOI: 10.1021/acscatal.9b04687
ACS Catal. 2020, 10, 1146−1151

(15) Dobbek, H.; Gremer, L.; Kiefersauer, R.; Huber, R.; Meyer, O. Catalysis at a dinuclear [CuSMo(=O)OH] cluster in a CO dehydrogenase resolved at 1.1-Å resolution. *Proc. Natl. Acad. Sci. U.S.A.* **2002**, *99*, 15971−15976.
(16) Clark, M. L.; Grice, K. A.; Moore, C. E.; Rheingold, A. L.; Kubiak, C. P. Electrocatalytic CO2 reduction by M(bpy-R)(CO)4 (M = Mo, W; R = H, tBu) complexes. Electrochemical, spectroscopic, and computational studies and comparison with group 7 catalysts. *Chem. Sci.* **2014**, *5*, 1894−1900.
(17) Ramos Sende, J. A.; Arana, C. R.; Hernandez, L.; Potts, K. T.; Keshevarz-k, M.; Abruna, H. D. Electrocatalysis of CO2 Reduction in Aqueous Media at Electrodes Modified with Electropolymerized Films of Vinylterpyridine Complexes of Transition Metals. *Inorg. Chem.* **1995**, *34*, 3339−3348.
(18) Pickett, C. J.; Pletcher, D. Electrochemical reduction of Group 6 metal hexacarbonyls in aprotic solvents. *J. Chem. Soc., Dalton Trans.* **1976**, *8*, 749−752.
(19) Maia, L. B.; Fonseca, L.; Moura, I.; Moura, J. J. G. Reduction of Carbon Dioxide by a Molybdenum-Containing Formate Dehydrogenase: A Kinetic and Mechanistic Study. *J. Am. Chem. Soc.* **2016**, *138*, 8834−8846.
(20) Tory, J.; Setterfield-Price, B.; Dryfe, R. A. W.; Hartl, F. [M(CO)4(2,2′-bipyridine)] (M=Cr, Mo, W) Complexes as Efficient Catalysts for Electrochemical Reduction of CO2 at a Gold Electrode. *ChemElectroChem* **2015**, *2*, 213−217.
(21) Grice, K. A.; Saucedo, C. Electrocatalytic Reduction of CO2 by Group 6 M(CO)6 Species without "Non-Innocent" Ligands. *Inorg. Chem.* **2016**, *55*, 6240−6246.
(22) Neri, G.; Donaldson, P. M.; Cowan, A. J. The Role of Electrode−Catalyst Interactions in Enabling Efficient CO2 Reduction with Mo(bpy)(CO)4 As Revealed by Vibrational Sum-Frequency Generation Spectroscopy. *J. Am. Chem. Soc.* **2017**, *139*, 13791−13797.
(23) Jiang, C.; Nichols, A. W.; Machan, C. W. A look at periodic trends in d-block molecular electrocatalysts for CO2 reduction. *Dalton Trans.* **2019**, *48*, 9454−9468.
(24) Francke, R.; Schille, B.; Roemelt, M. Homogeneously Catalyzed Electroreduction of Carbon Dioxide—Methods, Mechanisms, and Catalysts. *Chem. Rev.* **2018**, *118*, 4631−4701.
(25) Franco, F.; Cometto, C.; Sordello, F.; Minero, C.; Nencini, L.; Fiedler, J.; Gobetto, R.; Nervi, C. Electrochemical Reduction of CO2 by M(CO)4(diimine) Complexes (M=Mo, W): Catalytic Activity Improved by 2,2′-Dipyridylamine. *ChemElectroChem* **2015**, *2*, 1372−1379.
(26) Sieh, D.; Lacy, D. C.; Peters, J. C.; Kubiak, C. P. Reduction of CO2 by Pyridine Monoimine Molybdenum Carbonyl Complexes: Cooperative Metal−Ligand Binding of CO2. *Chem. - Eur. J.* **2015**, *21*, 8497−8503.
(27) Hooe, S. L.; Rheingold, A. L.; Machan, C. W. Electrocatalytic Reduction of Dioxygen to Hydrogen Peroxide by a Molecular Manganese Complex with a Bipyridine-Containing Schiff Base Ligand. *J. Am. Chem. Soc.* **2018**, *140*, 3232−3241.
(28) Nichols, A. W.; Chatterjee, S.; Sabat, M.; Machan, C. W. Electrocatalytic Reduction of CO2 to Formate by an Iron Schiff Base Complex. *Inorg. Chem.* **2018**, *57*, 2111−2121.
(29) Hooe, S. L.; Machan, C. W. Dioxygen Reduction to Hydrogen Peroxide by a Molecular Mn Complex: Mechanistic Divergence between Homogeneous and Heterogeneous Reductants. *J. Am. Chem. Soc.* **2019**, *141*, 4379−4387.
(30) Chapovetsky, A.; Do, T. H.; Haiges, R.; Takase, M. K.; Marinescu, S. C. Proton-Assisted Reduction of CO2 by Cobalt Aminopyridine Macrocycles. *J. Am. Chem. Soc.* **2016**, *138*, 5765−5768.
(31) Chapovetsky, A.; Welborn, M.; Luna, J. M.; Haiges, R.; Miller, T. F.; Marinescu, S. C. Pendant Hydrogen-Bond Donors in Cobalt Catalysts Independently Enhance CO2 Reduction. *ACS Cent. Sci.* **2018**, *4*, 397−404.
(32) Sathrum, A. J.; Kubiak, C. P. Kinetics and Limiting Current Densities of Homogeneous and Heterogeneous Electrocatalysts. *J. Phys. Chem. Lett.* **2011**, *2*, 2372−2379.
(33) Stiddard, M. H. B. 910. 2,2′-Bipyridyl derivatives of Group VI carbonyls. *J. Chem. Soc.* **1962**, 4712−4715.
(34) Kanthimathi, M.; Nair, B. U.; Ramasami, T.; Shibahara, T. Preparation, characterization and reactivities of chromium (III) complexes of a homologous series of Schiff-base ligands. *Chem. Sci.* **1997**, *109*, 235−248.
(35) Franco, F.; Pinto, M. F.; Royo, B.; Lloret-Fillol, J. A Highly Active N-Heterocyclic Carbene Manganese(I) Complex for Selective Electrocatalytic CO2 Reduction to CO. *Angew. Chem., Int. Ed.* **2018**, *57*, 4603−4606.
(36) Passard, G.; Dogutan, D. K.; Qiu, M.; Costentin, C.; Nocera, D. G. Oxygen reduction reaction promoted by manganese porphyrins. *ACS Catal.* **2018**, *8*, 8671−8979.
(37) Azcarate, I.; Costentin, C.; Robert, M.; Saveant, J. M. Through-Space Charge Interaction Substituent Effects in Molecular Catalysis Leading to the Design of the Most Efficient Catalyst of CO2-to-CO Electrochemical Conversion. *J. Am. Chem. Soc.* **2016**, *138*, 16639−16644.
(38) Costentin, C.; Passard, G.; Robert, M.; Savéant, J.-M. Ultraefficient homogeneous catalyst for the CO2-to-CO electrochemical conversion. *Proc. Natl. Acad. Sci. U.S.A.* **2014**, *111*, 14990.
(39) Riplinger, C.; Sampson, M. D.; Ritzmann, A. M.; Kubiak, C. P.; Carter, E. A. Mechanistic Contrasts between Manganese and Rhenium Bipyridine Electrocatalysts for the Reduction of Carbon Dioxide. *J. Am. Chem. Soc.* **2014**, *136*, 16285−16298.
(40) Sampson, M. D.; Kubiak, C. P. Manganese Electrocatalysts with Bulky Bipyridine Ligands: Utilizing Lewis Acids To Promote Carbon Dioxide Reduction at Low Overpotentials. *J. Am. Chem. Soc.* **2016**, *138*, 1386−1393.
(41) Rebelein, J. G.; Lee, C. C.; Hu, Y.; Ribbe, M. W. The in vivo hydrocarbon formation by vanadium nitrogenase follows a secondary metabolic pathway. *Nat. Commun.* **2016**, *7*, No. 13641.

DOI: 10.1021/acscatal.9b04687
ACS Catal. 2020, 10, 1146−1151